Proceedings World Geothermal Congress 2026
Calgary, Canada, June 8 – 11, 2026

Retrofitting Abandoned Slate Mine For Long-Term Thermal Energy Storage: Lessons Learned From the WeForming and Ard-Nrgy Projects

Frédéric Ransy[1]*, Aitor Cendoya[1] and Vincent Lemort[1]
University of Liege[1]*
*frederic.ransy@uliege.be

Keywords: UTES, Slate Mine, Energy efficiency, District heating, Energy Transition

ABSTRACT

This paper presents the lessons learned from the WeForming and Ard-Nrgy projects, which aim to convert a former slate mine in Martelange, Belgium, into a large-capacity underground thermal energy storage facility. Considering the European climate objectives and the growing need to integrate intermittent renewable energy sources into heating networks, the reuse of abandoned flooded mines represents an innovative technical and economic opportunity. After exploring the identified cavity and conducting drilling operations, a complete pumping, heat exchange, water treatment, and fiber optic measurement system was installed. Detailed dynamic modeling, based on Modelica and the IDEAS library, was conducted to analyze the performance of three different architectures: an individual geothermal heat pump system, a centralized system without storage, and a centralized system with storage. The simulations show that underground storage can improve photovoltaic self-consumption and energy self-sufficiency, while ensuring seasonal storage efficiency comparable to conventional UTES systems. The results also demonstrate the importance of adequately sizing the underground storage volume, which is essential for optimizing system costs and performance. The conclusion is that the geological uncertainty dominates techno-economic viability of mine-based UTES.

1 INTRODUCTION

Given the EU policy and strategy to achieve its 2030 climate targets, i.e., a 55% reduction in greenhouse gases compared to 1990 levels, it is necessary to develop technical solutions to decarbonize all sectors of the economy. The building heating and cooling sector is still a particularly significant source of greenhouse gas emissions. In this context, 4th and 5th generation heating and cooling networks are particularly interesting technologies, as they allow for the integration of various renewable and low-carbon thermal energy sources, such as waste heat, geothermal energy, biomass, and solar thermal energy. It also allows the integration of renewable electricity generation such as wind and photovoltaics through conversion technologies including heat pumps. However, some of these technologies are intermittent and seasonal, and the use of large-capacity underground thermal storage allows for better management of these intermittencies [1].

There are different types of Underground Thermal Energy Storage (UTES), characterized by different levels of maturity, efficiency, cost, and complexity [2,3]. The systems described in the literature are Aquifer Thermal Energy Storage (ATES), Borehole Thermal Energy Storage (BTES), Pit Thermal Energy Storage (PTES), and Mine Water Energy Storage (MWES).

The ATES system [4, 5] uses naturally occurring aquifers in the subsurface as a heat source and heat storage system. Temperature levels range from 5 to 25°C, with a cold well and a hot well. Seasonal storage efficiency generally ranges from 67 to 87%. Higher temperature operation (50°C) is also possible, but seasonal efficiency decreases significantly (40-70%), and the risk of clogging the production wells due to physical, chemical, or biological mechanisms increases significantly. Furthermore, an accurate assessment of hydrogeological conditions is necessary before any investment, in order to verify the technical and economic feasibility of the site.

The BTES system [6, 7, 8] stores heat directly in the ground using vertical probes placed in vertical boreholes. Typically, the depth varies from 30 to 200 meters, with a distance between probes of between 2 and 4 meters, depending on the thermal characteristics of the soil. These systems are usually connected to heat pumps to raise the temperature level, which is limited to 25-45°C 4-25°C at the system outlet. The BTES system must be properly sized according to the characteristics of the soil in order to achieve the desired performance, and a compromise must be found between thermal conductivity and storage capacity [9]. In addition, it takes several years for thermal equilibrium to be reached (if the heating and cooling loads are balanced), with seasonal storage efficiency typically reaching 40-60%. [10]

The PTES system [11] [12] [13] consists of an artificial excavated basin filled with water, with a volume ranging from 1,000 to 200,000 m^3. The sides are covered with a hydrophobic, insulating membrane, and the surface is covered with floating insulating panels to limit heat losses. It is the most cost-effective solution for storages above 10,000 m^3. The storage temperature varies from 30 to 90°C. The seasonal storage efficiency can reach 75-90% in large installations.

The lowest TRL system is MWES. It uses water accumulated in the galleries and tunnels of abandoned mines. Below 100 meters, the temperature is constant and increases with depth. This system requires an accurate estimation of the water flow rate and temperature that can be extracted, which depend on the configuration and permeability of the tunnels. With optimal conditions, the system offers a high water flow rate at a constant temperature. In the Netherlands, the Minewater 2.0 project in Heerlen [14] has demonstrated the technical and economic feasibility of using this resource to supply a 5th generation heating and cooling network.

In this context, the objective of the WeForming and Ard-Nrgy projects is to develop a prototype of an Underground Thermal Energy Storage in an abandoned slate mine in Martelange, Belgium. The site, which was previously used to produce slate, has been abandoned. Nowadays, the objective is to convert the site into an Underground Thermal Energy Storage. A second objective of the project, not described in this paper, is to develop a prototype of a reversible heat pump/ORC Carnot battery connected to the UTES. More information can be found in [15] and [16].

The purpose of this paper is to describe the progress of the project from the design and operational perspectives. The first section describes the case study. The second section explains the technology implemented for the Underground Thermal Energy Storage. The third and final section discusses the results obtained and proposes a technoeconomic simulation of this type of system.

2 DESCRIPTION OF THE CASE STUDY

As shown in Figure 2, the mine is located in southeastern Belgium, in the town of Martelange. The site, which was in operation between 1895 and 1995, extracted blocks of shale from a depth of 40 to 160 meters. The blocks were then brought to the surface to be cut and transformed into roofing slates. A large amount of waste, unsuitable for slate production, was left on the surface. Since 2021, this material has been used as natural stone for construction and gardening.

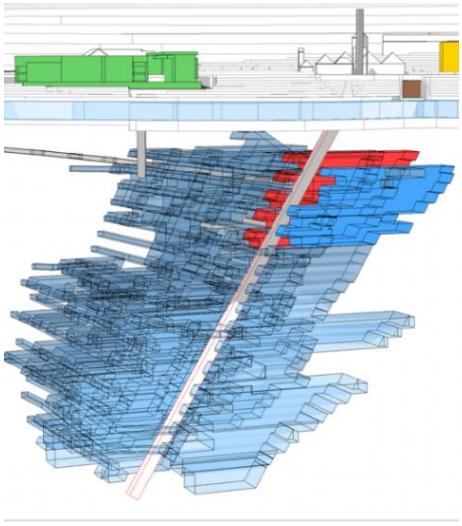

Figure 1: 3D representation of the UTES **Figure 2: Location of the UTES prototype**

Exploitation began with the six chambers closest to the surface, between -40 meters and -120 meters. They are 10 meters wide, 30 meters deep, and vary in height between 60 and 80 meters. Exploitation then continued with six deeper chambers, between -120 and -160 meters.

In order to minimize risks and costs, the cavity closest to the surface was selected as a prototype for the Underground Thermal Energy Storage. According to the historical underground mine plans, this cavity has a volume of 27.200 m^3 for an initial investment cost estimated at 400.000 €, representing a theoretical relative cost of 15 €/m^3, which is competitive compared to other UTES technologies. This represents the first step of the project.

The project also includes a second phase, which consists of the construction of an eco-neighborhood on the surface, comprising residential housing units, tertiary buildings, and small industry, for a total consumption of approximately 1.100 MWh of thermal energy. The objective is to connect this complex to the Underground Thermal Energy Storage in order to increase energy resilience and self-consumption, and minimize energy costs. In addition, buildings were built in 2019 on the site, and are heated by individual geothermal heat pumps using cold water from the mine as cold heat source.

Using technical and economic data collected during the first phase of the project, the paper proposes a techno-economic analysis of this type of underground thermal storage based on simulations parameterized with real project data.

3 DESCRIPTION OF THE UTES

The cavity initially chosen to be converted into underground thermal storage was first explored by divers to verify the dimensions indicated on the historical underground mine plans. The real dimensions are close to the latest known plans. However, it turned out that 75 % of the volume was in fact occupied by shale waste fill. During operation, a large amount of waste was dumped into this cavity instead of being left on the surface due to lack of space. As a result, the actual usable water volume is 6.500 m^3, instead of the expected 27.200 m^3.

Four vertical boreholes were drilled to access the cavities. Steel casing was installed along the entire height of each well. Two wells are used to extract hot water from the top of the cavity, one well is used to extract cold water from the bottom, and the last well is used to return hot or cold water to the center of the cavity using a diffusion system. The use of two production wells for hot water is justified by the V-shaped geometry of the cavity, which allows hot water to be extracted across the full width of the storage volume. This configuration promotes uniform flow distribution and helps maintain good temperature stratification within the storage facility. Submersible pumps, connected to insulated pipes, are placed in the steel pipes to create water flow. Figure 3 shows the underground storage facility and associated systems. The left-hand side shows a cross-section of the cavity, in orange, with the four wells. The upper part shows one of the submersible pumps and one of the production well access. The lower part shows the interior of the thermal storage facility, with an access tunnel filled with groundwater and the diffusion system.

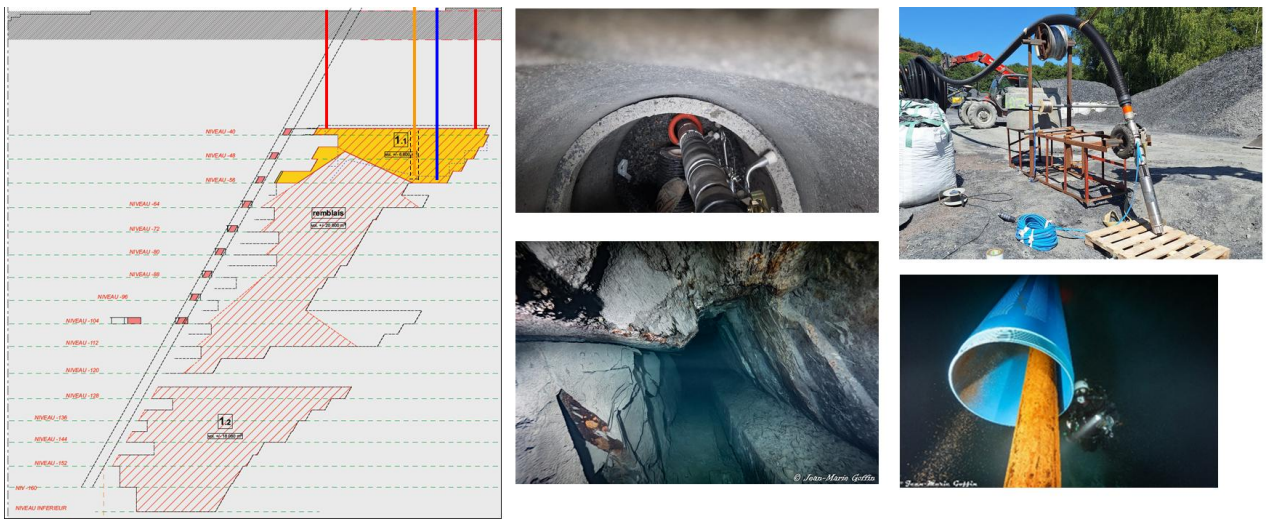

Figure 3: Representation of underground storage. Left: Cross-sectional plans with boreholes. Top: Underground pump outside and inside the access shaft. Bottom: Interior of the underground storage, with access tunnel and diffusion system.

Once the water has been extracted from the cavity, it is transported to the main technical building where the energy production systems are located, through a network of insulated, buried pipes. To prevent any contamination of the water, a plate heat exchanger is used to exchange heat between the underground storage facility and the energy production facility. In that way, the two hydraulic circuits (the mine and the energy production facility distribution network) are decoupled, with two different pressure values.

Numerous water samples identified a risk of fouling of heat exchangers during heating. For this reason, a filtration system was installed upstream of the main exchanger. This consists of a sand filter and water softeners.

In order to study the performance of the storage facility and determine its state of charge, another smaller borehole was drilled to install a fiber optic temperature sensor. This system allows the temperature to be measured throughout the entire height of the storage facility, in both the water and the rock.

The cost of the UTES can be divided into the following terms:

- Drilling to create production wells and install the fiber optic measurement system,
- Submersible pumps,
- All the insulated pipes used to transport water from the storage facility to the energy production facility,
- The water treatment system,
- The hydraulic unit, including the heat exchanger and other components,
- The fiber optic measurement system,
- Civil engineering associated with the production wells

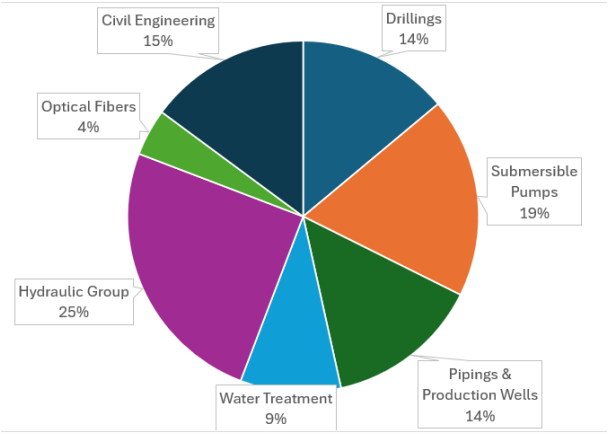

Figure 4: Cost repartition associated with the construction of UTES

The total construction cost of the UTES is 337.000 €. This cost is based on actual quotes obtained from the Ard-Nrgy and WeForming projects. Figure 4 shows the cost repartition associated with the UTES construction. The relative cost is 52 €/m^3, which is higher than initially estimated at the beginning of the project (15 €/m^3), but remains competitive compared to other underground thermal storage technologies. The reason for this price increase is the presence of shale waste in the cavity, reducing the effectively usable volume from 27.200 m^3 to 6.500 m^3.

4 RESULTS

4.1 Architectures considered

In order to demonstrate the benefits of UTES, a detailed semi-empirical dynamic model of the complete system was developed and presented in Modelica. This model calculates the system dynamic state, taking into account inertia and partial load performance. It is based on the geometry of its various components, such as the surface area of the exchangers, the storage volume, the subsurface properties, the technical characteristics of the photovoltaic panels, etc. The models (Photovoltaic panels, heat exchangers, pumps, heat pump, storage tank) are calibrated and validated with manufacturer technical data sheets.

Three architectures are proposed and compared: the "individual system" architecture (Case 1), the "centralized system without UTES" architecture (Case 2), and the "centralized system with UTES" architecture (Case 3). Figure 5, Figure 6, and Figure 7 represent these three architectures.

The "individual system" architecture (Figure 5) assumes that each building has its own geothermal heat pump for heating. This architecture is the one currently implemented. A building corresponds to a residential apartment building. Each heat pump uses cold water at 9°C from the mine as cold source. In addition, each building has a photovoltaic installation in addition to its residential connection to the electricity grid to supply the heat pump with electricity. This is the heating installation currently in place in new buildings constructed in 2019. Each heat pump has a heating capacity of 60 kW, and the photovoltaic panels have a peak power of 32 kW.

The "centralized system without UTES" architecture (Figure 6) considers that a total of 12 buildings, identical to those defined in the "individual system" architecture, are connected together through a heating network. This heating network is connected to a 15 m^3 buffer tank that connects two production assets: 250 kW of electric heating resistors and a 450 kW geothermal heat pump. The heat pump's cold source is cold water at 9°C from the mine. Unlike the hot-water configuration presented in Figure 7, this cold source is not used as a thermal storage system, but rather as a naturally regenerated geothermal source. The installation is connected to the medium-voltage grid with a power limited to 400 kW. In addition, a 200 kW peak installation of photovoltaic panels connected to a 120 kWh battery is considered for on-site electricity self-consumption.

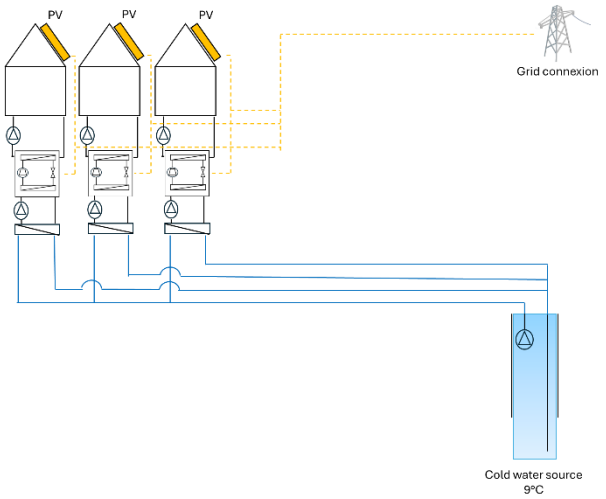

Figure 5: Architecture « individual system »

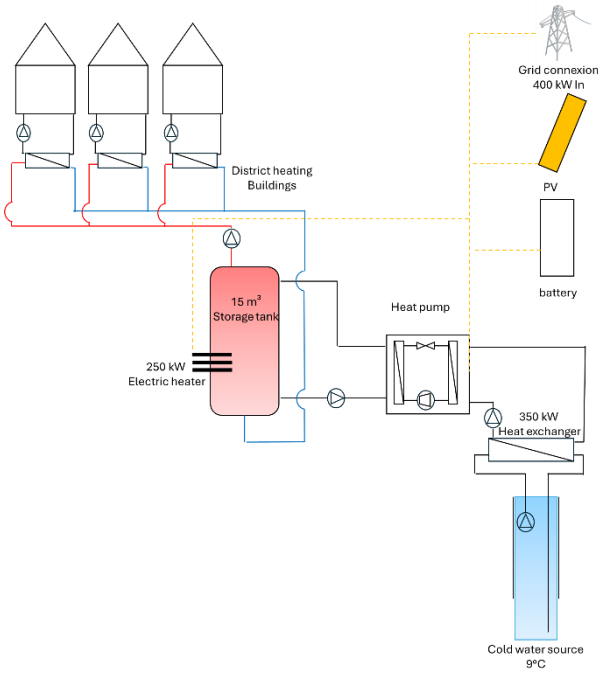

Figure 6: Architecture « centralized system without UTES »

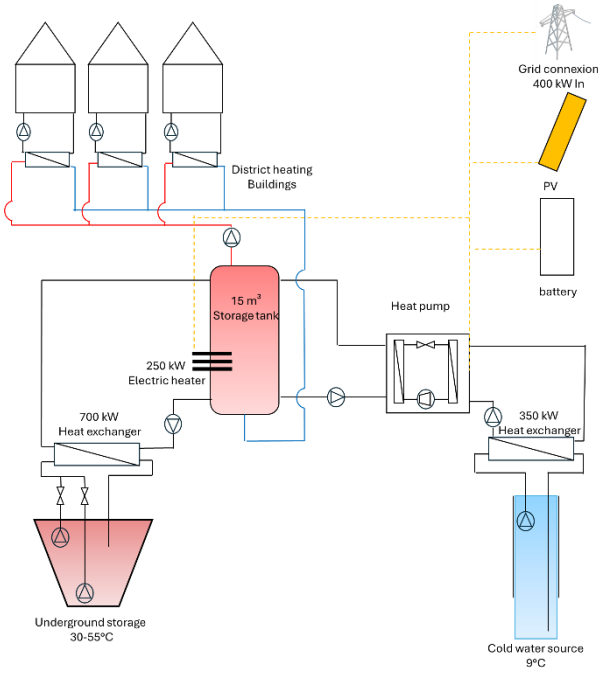

Figure 7 : Architecture « centralized system with UTES »

The "centralized system with UTES" architecture (Figure 7) is identical to the "centralized system without UTES" architecture, but the Underground Thermal Energy Storage is added to the system. The water temperature in this storage can vary from 30°C to 55°C. For this case, two simulations (A and B) are considered to show the impact of the sizing parameters. In simulation A, 10 buildings are considered, the heat pump heating capacity is fixed at 350 kW, the photovoltaic panels have 100 kW peak power, the battery capacity is set at 60 kWh, and the storage has a volume of 6.500 m^3. In simulation B, 12 buildings are considered, the heat pump heating capacity is fixed at 450 kW, the photovoltaic panels have 200 kW peak power, the battery capacity is 120 kWh, and the storage volume is 27.200 m^3, for the same cost. Simulation B represents an idealized design scenario assuming full cavity availability identified during preliminary mine surveys, rather than the currently accessible prototype volume. In this simulation B, the parameters, except for the storage, are identical to those of the "centralized system without UTES" architecture.

The reference building used to determine the 15-min heat consumption comprises 13 apartments, a basement (garage), and a "common" area with staircases providing access to the apartments. Table 1 summarizes all the characteristics of the building. It is an apartment building constructed in 2019, with a total heated area of 1.401 m^2 and a volume of 3.447 m^3. There are four floors with a total height of 12.2 meters. The thermal characteristics of the building envelope (U-Values) are also indicated. They correspond to an excellent level of thermal insulation. The infiltration rate under 50 Pa, n_{50} , is not known, but is estimated at 2 h^{-1}. The building's inertia is considered heavy, as the structure is made of concrete.

The ventilation system consists of an individual exhaust ventilation system, with fresh air supplied through ventilation openings above the windows and extracted by a central fan and an air duct network. The extracted air is used to supply an exhaust air heat pump in each apartment, which produces domestic hot water stored in a storage tank. The heat emission system consists of underfloor heating for each dwelling, supplied at a temperature of 35-25°C. An individual room thermostat regulates the flow of water circulating in the floor through a controllable valve at the inlet to the hydraulic circuit.

4.2 Modeling

The building and the heating production system are modeled using the Modelica simulation software and the IDEAS (Integrated District Energy Assessment Simulations) library. This open-source library has been developed since 2013 by KU Leuven. It enables detailed modeling of buildings, heat production and distribution systems. The library, described in [17], has been validated as part of the IBPSA project 1 and the "Twin house IEA EBC Annex 58" case studies.

The library uses an object-oriented approach. The complete system is divided into sub-components, which are modeled separately and then connected together. The outer envelope is defined first. The library allows the different materials constituting each wall (exterior, interior, roof, floor, etc.) to be encoded, taking into account conductivity and thermal inertia. This allows the energy stored in the walls to be accurately taken into account. In order to be sufficiently accurate, the building is divided into 15 separate interconnected zones: 13 occupied apartments, the unheated garage, and the unheated common areas. The models for each zone use components from the IDEAS library, including the zone model, window model, internal wall model, and external wall model. Each zone is then connected to its ventilation system. This involves constant air injection and extraction, with a fixed flow rate determined by the energy certificate (energy performance of buildings). Each zone is also connected to its own emission system, the underfloor heating. This is modeled using standard EN 15337 [18] and is described in [19]. The inertia of the materials constituting the underfloor heating is also taken into account. Finally, each zone is connected to a thermostat that regulates the water flow in each underfloor heating system. The set-point temperature is fixed between 20 and 22°C in winter and 25°C in summer.

Table 1: Characteristics of the building

General Building Information		
Parameter	**Description/value**	**Unit**
Building type	Multi-family	-
Construction year	2019	-
Location	Martelange	-
Heat floor area	1401	m^2
Heated volume	3447	m^3
Number of floors	4	-
Building height	12.2	m
Envelope characteristics		
Parameter	**Value**	**Unit**
Wall U-Value	0.19	W/m^2K
Roof U-Value	0.16	W/m^2K
Floor U-value	0.21	W/m^2K
Window U-Value	1.4	W/m^2K
Solar heat gain coeff.	0.63	-
Window-to-Wall ratio	32	%
Infiltration n_{50}value (estimation)	2	h^{-1}

Thermal demand of the buildings being known, it is necessary to determine the efficiency of the heat production system using a detailed model. This work is carried out for the three architectures (Figure 5, Figure, and Figure).. The following physical principles are considered:

- The heat pump model takes into account the variation of the COP and the heating capacity with the operating conditions, i.e., the inlet temperatures of the water in the condenser and the evaporator. These values are based on available manufacturer data.
- The exchanger model takes into account variations in thermal efficiency depending on operating conditions, i.e., the temperatures and flow rates of each fluid. Performance under nominal operating conditions is imposed using manufacturer data. Inertia is also taken into account in order to correctly model the shutdown and start-up phases.
- The storage tank model takes into account water stratification, using discretization into several identical volumes, and also calculates heat losses to the outside environment.
- Pump consumption is determined based on water flow rates, pressure drop in each circuit, and the hydraulic and electrical efficiency of each pump and associated motor.

To model the electricity production of photovoltaic panels, the "photovoltaic-thermal collector" component of the IDEAS library is used. This model includes a module for electricity production. The model uses the "PVWatts v5 methodology" [20], and has been experimentally validated in [21]. The model parameters are the nominal power, the temperature coefficient, the surface area, and the efficiency of the panel.

The underground storage model uses the MoSDH library [22], adapting an existing validated model. Figure 6 shows the model, which has two components: the soil model, using an R-C network, and the water volume model, discretized into several layers.

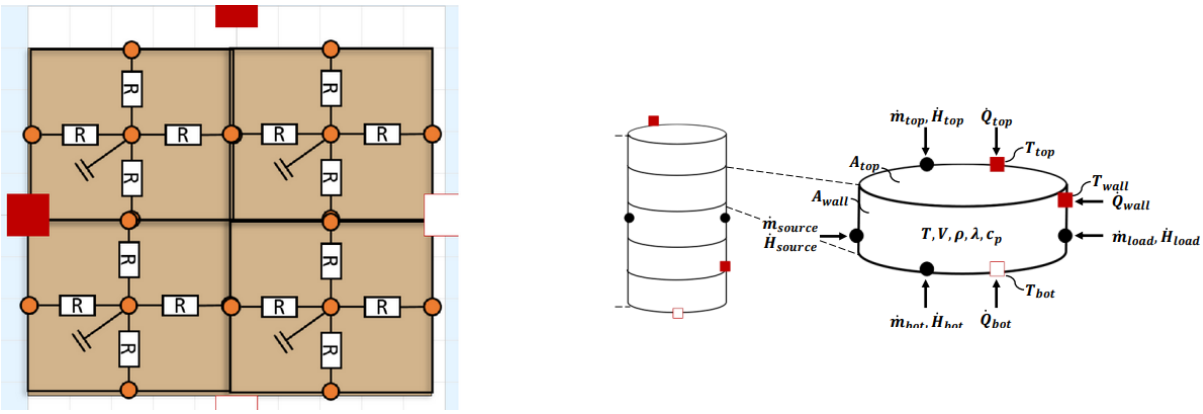

Figure 6: Underground storage modeling. R-C network (left). Water volume model (right).

4.3 Performance Indicator

The model described in the section 4.2 can be used to determine the following 15-min power exchanges:

- The thermal demand of the building(s), denoted $\dot{Q}_{buildings}$,
- The electrical power produced by the photovoltaic panels, denoted $\dot{W}_{PV}$,
- The electrical power consumed by the building(s), denoted by $\dot{W}_{load}$,
- The thermal power injected into and withdrawn from the Underground Thermal Energy Storage, denoted by $\dot{Q}_{sto,in}$ and $\dot{Q}_{sto,out}$,

The electrical power produced by the photovoltaic panels is divided into two parts: the self-consumed part, denoted $\dot{W}_{PV,SC}$, and the part fed back into the electrical grid. These terms are calculated as follows:

$$\dot{W}_{PV,SC} = \min(\dot{W}_{PV}, \dot{W}_{load}) \quad (1)$$

$$\dot{W}_{PV,out} = \dot{W}_{PV} - \dot{W}_{PV,SC} \quad (2)$$

The electrical power consumed directly from the grid is denoted as $\dot{W}_{in,grid}$, and is calculated as follows:

$$\dot{W}_{in,grid} = \dot{W}_{load} - \dot{W}_{PV,SC} \quad (3)$$

The thermal and electrical powers are then integrated over time to obtain the annual energies, $Q_{buildings}$, $W_{PV,SC}$, W_{PV}, W_{load}, $Q_{sto,out}$ and $Q_{sto,in}$, expressed in MWh. The following performance indicators are then defined:

$$SPF = \frac{Q_{buildings}}{W_{load}} \quad (4)$$

$$SCR = \frac{W_{PV,SC}}{W_{PV}} . 100 \quad (5)$$

$$SSR = \frac{W_{PV,SC}}{W_{load}} . 100 \quad (6)$$

$$\varepsilon_{sto} = \frac{Q_{sto,out}}{Q_{sto,in}} \quad (7)$$

The term SPF represents the seasonal production efficiency of the heat production system, calculated as the ratio of the annual energy supplied to the buildings, $Q_{buildings}$, to the total electricity consumption, W_{load} . The self-consumption ratio (SCR) represents the percentage of photovoltaic energy produced that is consumed directly on site. The self-sufficiency ratio (SSR) represents the percentage of the site consumption that is supplied directly by local photovoltaic energy. Ideally, a system based on renewable energy sources should approach self-consumption and self-sufficiency ratios of 100%. Finally, the term ε_{sto} represents the annual

efficiency of underground thermal storage, calculated as the ratio of the energy extracted from storage ($Q_{sto,out}$) to the energy supplied to it ($Q_{sto,in}$).

The final performance indicator is the cost of thermal energy supplied (COE), expressed in €/MWh:

$$COE = CAPEX+OPEX \quad (8)$$

Where COE refers to the cost of energy, CAPEX refers to investment costs, and OPEX refers to costs related to operating the system. CAPEX costs are calculated using the following simplified formula:

$$CAPEX = \frac{C_0 \psi}{Q_{buildings}} \quad (9)$$

$$\psi = \frac{i}{1-(1+i)^{-N}} \quad (10)$$

Where C_0 is the initial investment cost for the complete system, ψ the annuity factor, i the interest rate fixed at 4 %, and N is the system's lifespan, considered to be 25 years. The batteries are considered to be replaced after 12.5 years. The initial investment costs are detailed below for each of the architectures. These values are based on actual data from the WeForming project. OPEX operating costs are calculated as follows:

$$OPEX = \frac{C_{el}+C_{O\&M}+C_{fixed}}{Q_{buildings}} \quad (11)$$

Where C_{el} denotes the total annual cost of electricity consumed from the grid (energy-based costs), $C_{O\&M}$ denotes the annual cost of operation and maintenance, and C_{fixed} are the fixed annual costs. These costs are detailed below for each architecture considered. These values are based on real data from the WeForming project. The investment costs are as follows. For case 1 (Figure 5), the cost is 144.200 € per building. For case 2 (Figure 6), the cost is 1.401.748 € for the entire system. For case 3 (Figure 7), the cost is 1.555.374 € for case A, and 1.738.748 € for case B.

The operating costs are as follows. For case 1 (Figure 5), the price of electricity is fixed at the "residential customer" price for November 2025, i.e., 360 € MWh, fixed. Maintenance costs are fixed at 882 €/year per building. Fixed costs are equal to zero for that configuration. For cases 2 and 3 (Figure 6 and Figure 7), the annual operation and maintenance costs are fixed at 1.5 % of the total capital cost. The fixed costs are 20.000 €/year for the DSO peak demand charges, and 20.000 €/year for the regional tax and the market operation costs. The energy-based costs are divided into two terms: the dynamic electricity price and the distribution and transmission network charges. The 15 min Belgian day-ahead market is considered for the dynamic electricity price, and the distribution and transmission network charges are imposed at 75 €/MWh. Case 1 represents a residential tariff framework, while Cases 2–3 assume a district operator with market access.

4.4 Results

Table 2 summarizes the results obtained for the four simulations. Case 1 (individual system) shows good annual efficiency, with a system SPF of 4.2. In addition, annual photovoltaic production is significant, at 29 MWh, and theoretically sufficient to cover the annual consumption of 23 MWh. However, in reality, most of the photovoltaic production, 27 MWh, is fed back into the grid because it is produced at the wrong time. This results in very poor self-consumption and self-sufficiency ratios of 4.7% and 6%. The system is therefore highly dependent on the electricity grid for its energy supply. The cost of energy is 188 €/MWh, of which 52 % is CAPEX and 48 % is OPEX.

Case 2 (centralized system without UTES) has a lower system SPF of 3.45 compared to case 1. This is due to the higher temperature required at the heat pump outlet to supply the heating network, the heat losses from the network, and the use of electric heating resistors to cover peak demand. Despite this, the energy price is lower, at 175 €/MWh, of which 45 % is CAPEX and 55 % is OPEX. This is explained by the reduction in CAPEX achieved through economies of scale, which reduce the cost per kW installed as installed capacity increases, and by the reduction in OPEX achieved through variable prices and greater self-consumption of cheaper photovoltaic energy produced on site. Thanks to the battery, self-consumption and self-sufficiency stand at 46 % and 25 %.

Case 3 (centralized system with UTES), simulation A, is an example of poor design. Despite the integration of the underground storage, the cost of energy is 204 €/MWh, of which 51 % is CAPEX and 49 % is OPEX. In this design, the additional cost of storage is not compensated by a sufficient reduction in OPEX. This is because the storage volume is too small, meaning that the system is unable to store photovoltaic energy and capture sufficiently low energy prices. On the other hand, underground storage achieves a seasonal efficiency of 67%, which is

competitive with other available technologies. The problem with this design is therefore the UTES cost per m^3, which is too high.

Table 2 : Results for the 4 simulations considered

	Case 1	Case 2	Case 3 Simulation A	Case 3 Simulation B
$Q_{buildings}$ [MWh]	95	1140	950	1140
W_{load} [MWh]	23	330	363	439
W_{PV} [MWh]	29	175	87.5	175
W_{grid} [MWh]	21	250	294	265
SPF [-]	4.2	3.45	2.6	2.6
SCR [%]	4.7	46	79	100
SSR [%]	6.0	25	19	40
CAPEX [€/MWh]	98	79	105	98
OPEX [€/MWh]	90	96	99	85
COE [€/MWh]	188	175	204	183
$Q_{sto,in}$ [MWh]	0	0	680	948
$Q_{sto,out}$ [MWh]	0	0	459	647
ε_{sto} [%]	-	-	67	68

Case 3 (centralized system with thermal storage), simulation B, is more interesting. It considers a larger storage volume (27.200 instead of 6.500 m^3) for the same investment cost. In this case, the energy price is 183 €/MWh, of which 53 % is CAPEX and 47 % is OPEX. Although this case is 4 % more expensive than case 2, it has many advantages. Self-consumption and self-sufficiency increase to 100% and 40%, respectively. These values could be further increased by considering a higher installed photovoltaic capacity, which should further reduce the total cost of energy. In addition, CAPEX represents a relatively larger share of the energy price, which is more comfortable for end customers and investors. The annual efficiency of thermal storage is 68%, which is an acceptable value. These simulations demonstrate the importance of correctly sizing the various systems, including UTES, heat pumps, heating network, electric resistors, photovoltaic panels, and electric battery. To do this, an exploratory study is necessary before any investment is made to accurately determine the volume available in UTES, as well as its geological characteristics, in order to estimate the cost per m^3 with sufficient accuracy, as this parameter is essential for determining the final price of energy.

5 CONCLUSION

The analyses carried out as part of the WeForming and Ard-Nrgy projects demonstrate that converting a former slate mine into UTES is a credible solution for supporting the local energy transition. The storage studied has a seasonal efficiency of around 67-68%, which is comparable to the performance observed for other large-scale UTES technologies. However, the results highlight that economic viability is highly dependent on the volume actually accessible in the cavity. The unexpected reduction in usable volume due to shale backfill increased the cost per m^3, affecting the final price of energy. Simulations confirm that integrating storage into a centralized architecture improves photovoltaic self-consumption and self-sufficiency, thereby reducing dependence on the electricity grid, particularly when the storage volume is sufficient to capture energy during periods of low prices. Design B, incorporating a volume of 27.200 m^3 for the same CAPEX, shows a better balance between costs and performance, illustrating the importance of thorough exploration of cavities before any investment. The results show that the overall efficiency of such a system also depends on the correct sizing of the heat pump, photovoltaic peak power, electric battery capacity, and heating network. In conclusion, old mines are an interesting geological resource for creating competitive seasonal thermal storage, provided that a rigorous approach to exploration, modeling, and technical and economic optimization is adopted.

Acknowledgements

The authors would like to acknowledge the funding provided by the European Union's Horizon Research and Innovation program under grant agreement No. 10112355, in the framework of the WeForming project, and the funding provided by the Walloon Region of Belgium in the framework of the ARDNrgy project.

REFERENCES

[1] Guelpa, E., & Verda, V. (2019). Thermal energy storage in district heating and cooling systems: A review. *Applied Energy*, 252, 113474.

[2] Matos, C.R., Carneiro, J.F., & Silva, P.P. (2019). Overview of large-scale underground energy storage technologies for integration of renewable energies and criteria for reservoir identification. *Journal of Energy Storage*, 21, 241-258.

[3] Mahon, H., O'Connor, D., Friedrich, D., & Hughes, B. (2022). A review of thermal energy storage technologies for seasonal loops. *Energy*, 239, 122207.

[4] Fleuchaus, P., Godschalk, B., Stober, I., & Blum, P. (2018). Worldwide application of aquifer thermal energy storage: A review. *Renewable and Sustainable Energy Reviews*, 94, 861-876.

[5] Vukelić, Ž., Kumić, I., & Leko-Kos, M. (2024). Environmental and economic feasibility of high-temperature aquifer thermal energy storage. Renewable and Sustainable Energy Reviews, 189, 113898.

[6] Lanahan, M., & Tabares-Velasco, P.C. (2017). Seasonal thermal-energy storage: A critical review on BTES systems, modeling, and system design for higher system efficiency. *Energies*, 10(6), 743.

[7] Rad, F.M., & Fung, A.S. (2016). Solar community heating and cooling system with borehole thermal energy storage: Review of systems. *Renewable and Sustainable Energy Reviews*, 60, 1550-1561.

[8] Sadeghi, H., Jalali, R., & Singh, R.M. (2024). A review of borehole thermal energy storage and its integration into district heating systems. *Renewable and Sustainable Energy Reviews*, 192, 114236.

[9] Fogelström, E., Peñalosa, E., & Røkenes, K. (2024). Cost-optimal design of a seasonal borehole thermal energy storage system. Renewable Energy, 222, 119905.

[10] Gao, L., Zhao, J., & Tang, Z. (2015). A review on borehole seasonal solar thermal energy storage. *Energy* Procedia, 70, 209-218.

[11] Dahash, A., Ochs, F., Janetti, M.B., & Streicher, W. (2019). Advances in seasonal thermal energy storage for solar district heating applications: A critical review on large-scale hot-water tank and pit thermal energy storage systems. *Applied Energy*, 239, 265-294.

[12] Novo, A.V., Bayon, J.R., Castro-Fresno, D., & Rodriguez-Hernandez, J. (2010). Review of seasonal heat storage in large basins: Water tanks and gravel-water pits. *Applied Energy*, 87(2), 390-397.

[13] Bott, C., Dressel, I., & Bayer, P. (2019). State-of-technology review of water-based closed seasonal thermal energy storage systems. *Renewable and Sustainable Energy Reviews*, 113, 109241.

[14] Verhoeven, R., Willems, E., Harcout-Menou, V., De Boever, E., Hiddes, L., Op't Veld, P., & Demollin, E. (2014). Minewater 2.0 project in Heerlen the Netherlands: Transformation of a geothermal mine water pilot project into a full scale hybrid sustainable energy infrastructure for heating and cooling. Energy Procedia, 46, 58-67.

[15] Cendoya A., Ransy F., Guo B., Hernandez A., Dumont O., Lemort V. (2026). Design and modelling of a reversible HP/ORC Carnot battery tailored for waste heat integration in flooded mines, *Applied Energy*, Vol. 404, 127127, ISSN 0306-2619, https://doi.org/10.1016/j.apenergy.2025.127127.

[16] Cendoya, A., Ransy, F., Lemort, V., Hernandez, A., Dewallef, P., Gresse, P.-H., & Windeshausen, J. (2024). Modelling and simulation of a Carnot battery coupled to seasonal underground stratified thermal energy storage for heating, cooling and electricity generation. *Proceedings of the 20th International Refrigeration and Air Conditioning Conference at Purdue*, Paper 472.

[17] F. Jorissen, G. Reynders, R. Baetens, D. Picard, D. Saelens, and L. Helsen. (2018). Implementation and verification of the IDEAS building energy simulation library, *Journal of Building Performance Simulation*, vol. 11, no. 6, pp. 669–688.

[18] EN 15377. (2018). Heating systems in buildings – Design of embedded water-based surface heating and cooling systems.

[19] M. Koschenz and B. Lehmann (2000) *Thermoaktive Bauteilsysteme tabs. Dübendorf, Switzerland: EMPA Energyiesysteme/Haustechnik*, ISBN: 9783905594195.

[20] Dobos, A. P. (2014). PVWatts Version 5 Manual. NREL/TP-6A20-62641

[21] Meertens, L., Jansen, J., Helsen, L. (2025). Development and Experimental Validation of an Unglazed Photovoltaic-Thermal Collector Modelica Model that only needs Datasheet Parameters, *16th International Modelica & FMI Conference*, Lucerne, Switzerland, Sep 8–10, 2025

[22] J. Formhals (2022). Object-oriented modeling of solar district heating systems with underground thermal energy storage. Dissertation, Technical University of Darmstadt, 2022.